DESIGN AND EVALUATION OF A NEW X-RAY DIFFRACTION TOPOGRAPH CAMERA

by

MARK JEROME DREILING

B. S., Kansas State University, 1962

A MASTER'S THESIS

submitted in partial fulfillment of the

requirements for the degree

MASTER OF SCIENCE

Department of Physics

KANSAS STATE UNIVERSITY
Manhattan, Kansas

1964

Approved by:

R. Dean Dragsdorf
Major Professor

TABLE OF CONTENTS

INTRODUCTION

In this research an attempt was made to construct an x-ray diffraction topograph camera. The camera was to be especially suited for use with the microfocus x-ray source and have several characteristics which are improvements over existing units.

An x-ray diffraction topograph may be described as a mapping of the point to point variations of reflecting power by a nearly perfect single crystal. These variations are caused by changes in interplanar spacing or curvature of the lattice planes. Effects of this type are to be expected in the strain fields around dislocations, grain boundaries, slip planes, precipitates and other imperfections in the crystalline lattice.

The variations in intensity may be seen when a single crystal is aligned in a divergent beam. This is shown on Plate I, Fig. 1. Figure 1a shows the crystal as viewed parallel to the diffracting planes and perpendicular to the direction of the incident beam. Planes in one portion of the crystal are in position for diffraction. These are the planes which are set at the proper angle to satisfy the Bragg equation. Assuming monochromatic radiation and a perfect crystal, the diffracted image will appear as a trapezoid on the film. This is shown on Plate I, Fig. 1b. If the diffracting planes are nearly perpendicular to the surface of the crystal the paths

EXPLANATION OF PLATE I

Fig. 1a. A view of the diffracting crystal showing the width of the diffracted beam.

Fig. 1b. The source of the trapezoid on the film. A narrow beam incident from the left is diffracted from the set of planes perpendicular to H.

Fig. 1c. The source of the magnification factor obtained with the divergence of the incident beam.

Fig. 2. This is a view of a crystal showing extinction and diffraction from a distorted part of the lattice. The left hand diffracted beam is from the perfect portion and shows extinction. The diffracted beam interferes destructively with the incident beam to cause a loss in intensity in the diffracted beam. The right hand beam is incident at a slightly different angle and diffracts from tilted lattice planes and from planes with reduced d-spacings. This diffracted beam is not attenuated by interference from multiple reflections.

PLATE I

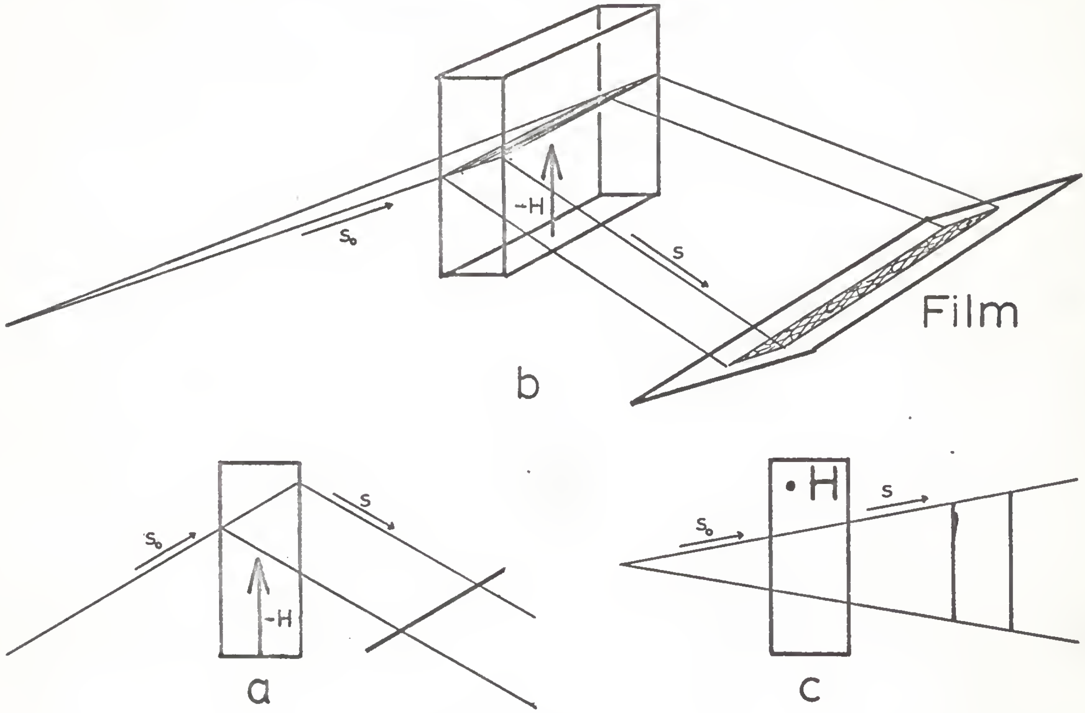

Figure 1

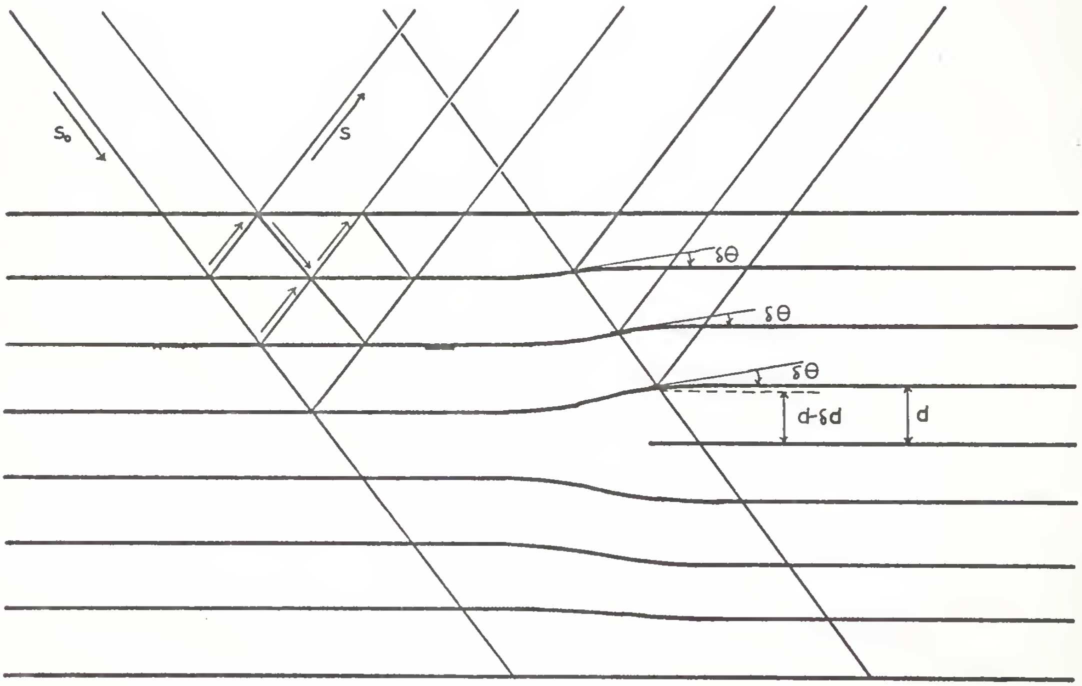

Figure 2

of all of the diffracted rays are equal within the crystal. For this case the exposure across the trapezoid will be nearly uniform.

If the variation of interplanar spacing or curvature of lattice planes exist along the diffracting zone, the intensity of the exposed area will be non-uniform. This non-uniformity has been observed extensively by A. R. Lang. In his experiments the crystal and film were translated stepwise in the beam to obtain successive trapezoids corresponding to several sections of the crystal. It was found that exposures from neighboring portions of the crystal were closely related. Extension of details was noted between the successive areas of exposure. This type of topograph was termed "section topograph" by Lang[1].

A feature of the section topograph is the magnification of the image in the direction parallel to the diffracting planes. This is illustrated in Plate I, Fig. 1c. This view perpendicular to the diffracting planes shows that the divergence of the incident beam is responsible for the magnification.

There is an increase in intensity of diffracted radiation from the distorted portions of the crystal. The reason for this increase is given by extinction arguments. Extinction refers to the loss of intensity in the diffracted beam due to interference between the primary and diffracted rays within the crystal. This occurs in perfect crystals when the incident beam is in position for diffraction. The diffracted beam sets up multiple reflections within the lattice which may interfere destructively with the incident and initially diffracted beams. This is shown on the left side of Plate I, Fig. 2. The right side of Fig. 2 shows the diffraction from a distorted part of the lattice. The incident beam, which is slightly divergent, has components which are in position to diffract from the perfect portions of the crystal. This diffracted beam is lowered in intensity due to extinction. Other components, however, will enter the crystal at an angle slightly different than the Bragg angle. These will not diffract from the perfect portion but may be in position to diffract from the distorted region. In this region the distortion may take the form of curvature of lattice planes or variation of interplanar spacing. Either of these may satisfy the Bragg condition for the incident components. If this is true, the diffracted beam will pass through the crystal to the film without setting up multiple reflections. As a result the diffracted beam from the distorted portion of the crystal will be more intense than that from the perfect portion.

A condition is placed on the increase in intensity from the distorted region. This condition is that the product μt, where μ is the linear absorbtion coefficient and t is the thickness of the crystal, be much less than unity. Only if this condition is fulfilled can there be sufficient contrast from imperfect regions. If the value of μt is greater than or equal to unity the contrast will be lowered or eliminated. For large values of μt the anomalous absorbtion effect will develop and the contrast variations will reverse to give less intensity from the distorted regions.

LANG METHOD

The section topograph was extended by Lang[1] by providing for continuous translation of the crystal and film through the beam. This had the effect of connecting all sections into one uniform picture. The experimental arrangement is shown in Fig. 1.

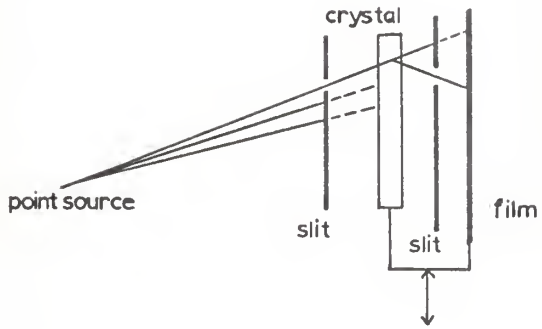

Fig. 1

The crystal is cut so that the diffracting planes make an angle of nearly 90° with the surface. This allows for uniform exposure and eases the construction of the equipment. The crystal and film are attached to the same arm which translates back and forth in the incident beam so that the crystal is always in position for diffraction. A stationary (with respect to the x-ray source) system of slits is employed to eliminate the unwanted characteristic radiations such as the K_{α_2} and K_β . The first slit is used to limit horizontal divergence of the incident beam. This is discussed later when resolution is considered. The slit after the crystal is used to stop the transmitted beam and to allow only the desired diffracted wavelengths to reach the film. The first slit, in conjunction with the crystal, acts to select the desired wavelengths.

As the crystal is translated, the images of the imperfections in the crystal will be projected onto the film. The projection is taken in the direction of the diffracted beam. This may be seen in Plate II, Figs. 1a and 1b. As the crystal and film are translated in the beam, the points 1 to 4 are matched with corresponding points on the film. The line imperfection along these points will show as a projection from the direction of the diffracted beam. As the crystal is translated from its position in Fig. 1a to its position in Fig. 1b, the correspondence between the points will be maintained.

The property of projection of imperfections is very important in the determination of the direction of dislocations within the crystal. A three dimensional model of the line imperfections can be constructed from two topographs taken from two different angles. The most convenient

EXPLANATION OF PLATE II

Fig. 1a Points on a line imperfection in a crystal being projected onto the film by diffraction.

Fig. 1b The same crystal after being translated with the film. The point to point relationship between crystal and film is maintained.

Fig. 2a The crystal in position for diffraction from one set of planes.

Fig. 2b The same crystal rotated through twice the Bragg angle to diffract off of the opposite side of the same set of planes. Two different projections are obtained.

PLATE II

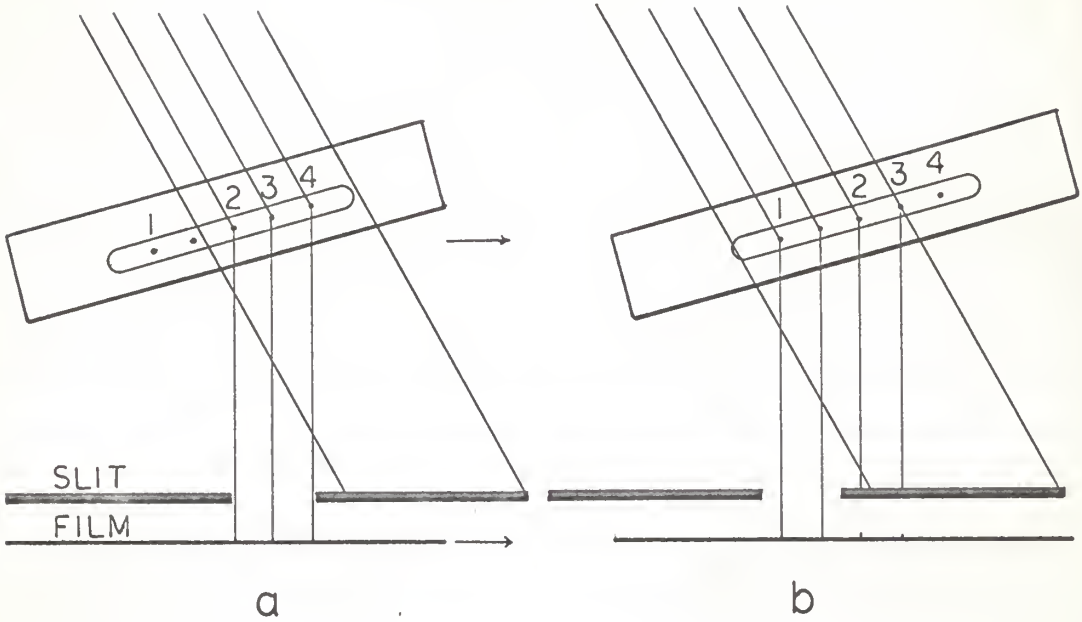

Figure 1

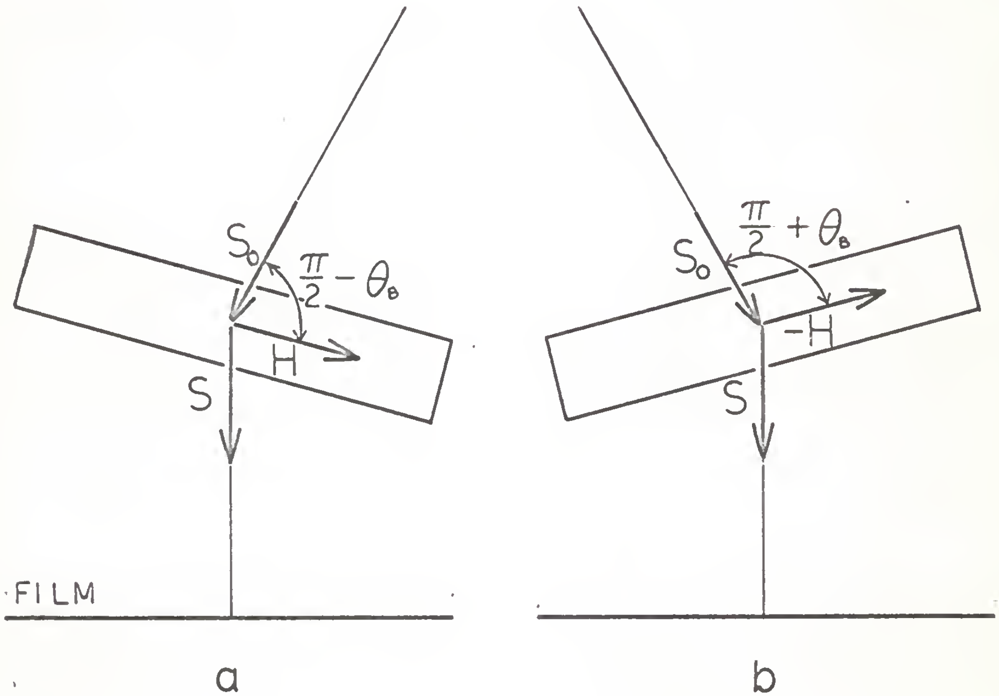

Figure 2

way to do this is to rotate the crystal through twice the Bragg angle to obtain the $(\overline{hkl})$ reflection. This is shown in Plate II, Figs. 2a and 2b. Here H represents the normal and the diffracting planes. It is seen that two projections are obtained which differ from each other in viewing angle by twice the Bragg angle. If the Bragg angle is small the images may be viewed with a stereo viewer. Otherwise a geometrical construction may be used.

Resolution is important because the images of single dislocations range in size from 5 microns to 20 microns. The resolution obtained depends principally upon two factors: the horizontal divergence and the vertical divergence of the x-ray beam incident on the crystal.

The vertical divergence effect is illustrated below in Fig. 2. Radiation from all points on the line source are in position to diffract from one point on the crystal plane. The point to point correspondence between the crystal and its film representation is lost. The image size is given by the formula $W' = (D'/D)W$. The resolution is improved by placing the source a long way from the crystal and moving the film very close to the crystal.

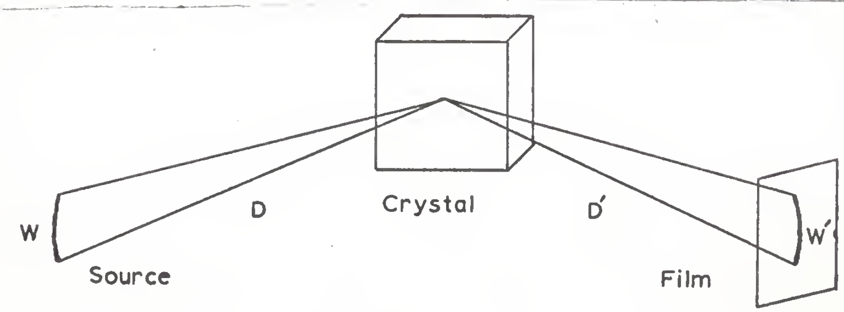

Fig. 2

The horizontal divergence depends on the horizontal width of the source. If the horizontal width of the source produces 100 sec of arc of divergence both the K_{α_1} and K_{α_2} may be diffracted from the same point in the crystal. A diagram of this effect is seen in Fig. 3. The two images will be separated by a distance W'' given by the formula W'' = D'' $(\Delta\lambda/\lambda)\tan\theta$. This problem was solved by Lang by using the first slit along with a large distance between the slit and the x-ray source to obtain a narrow beam.

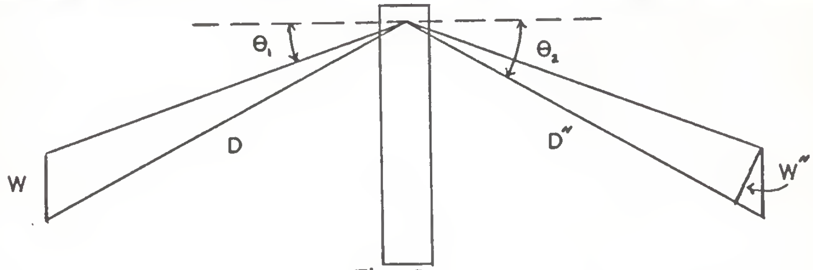

Fig. 3

A resolution of 4 microns has been obtained with the Lang technique in both the vertical and horizontal directions[5]. Exposure times vary between 10 and 60 hours depending on the radiation used, thickness of the sample, the value of ut and the set of planes used for diffraction.

The principal results obtained with the method are given by Lang[1] and Jenkinson[4]. They used AgK_{α_1} characteristic radiation and a thin silicon slice cut from a nearly perfect single crystal. The slice was cut parallel to the (111) planes. The (111) and (220) planes were used for diffraction. Imperfections appear in high contrast to the background and were positively identified as slip planes and dislocations. Specific types of dislocation interactions were observed in these topographs.

There are difficulties in aligning the Lang camera and results are difficult to reproduce. The Lang translation method is very sensitive to curvature of the sample[4]. The crystal generally must be remounted to obtain a stereo pair.

OBJECTIVES IN THE DESIGN OF A CAMERA

In consideration of these factors involving resolution and exposure time it was decided to design a topograph camera which would use to advantage the characteristics of the Hilger microfocus x-ray source.

The first objective of this work was to use the high specific intensity of the microfocus x-ray beam to obtain shorter exposure times. This higher intensity could also be used to advantage in alignment since adjustment can be checked quicker with the shorter exposure times available. The fact that the radiation from the microfocus unit is divergent and originates in a nearly point source was to be utilized also. The divergence of the beam may be used to select planes of diffraction and to obtain a magnification factor in one dimension. The small size of the source reduces the problem of horizontal divergence considerably. The general objective was to design a camera which would rotate the crystal in a divergent beam to select successive sections. This is the same as the Lang experiment except that rotation instead of translation is used to scan the crystal. The need for a narrow incident beam is eliminated because of the small size of the source.

ACTUAL DESIGN OF THE CAMERA

A method for obtaining topographs of crystals using a divergent beam was conceived by Dr. Dragsdorf. This section is concerned with the geometrical design of the camera.

The most important feature of the camera is the selection of planes in the divergent beam. This is illustrated in Plate III, Fig. 1. A crystal, with the plane normal H in the plane of the paper, is set to rotate about the axis A. The position of the diffracting region will be determined by the position of the crystal in its rotation about A.

If the diffracted beam is traced back through the crystal from any two diffraction positions, a virtual focus will be located. This virtual focus will remain nearly stationary for small angles of rotation of the crystal. The position of the virtual source is shown in Plate III, Fig. 2.

The stationary virtual source is invaluable in the design of the camera. It provides a reference point for the angular motion of the diffracted beam. The diffracted beam moves through an angle of $2\delta\theta$ for a rotation of the crystal of $\delta\theta$ about the axis A. This indicates that the motion of the

EXPLANATION OF PLATE III

Fig. 1 A crystal in a divergent x-ray source set to rotate about the axis A. The diffracting planes are parallel to A and only those in one section of the crystal are in position to diffract for a given crystal orientation.

Fig. 2 The same crystal in two diffracting positions. The diffracted rays are traced back through the crystal to locate the virtual source.

PLATE III

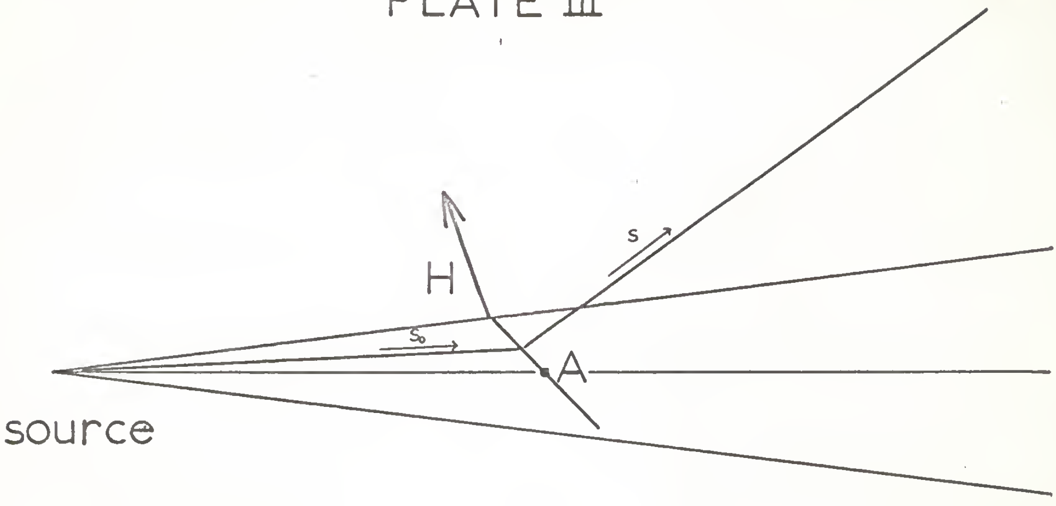

Figure 1

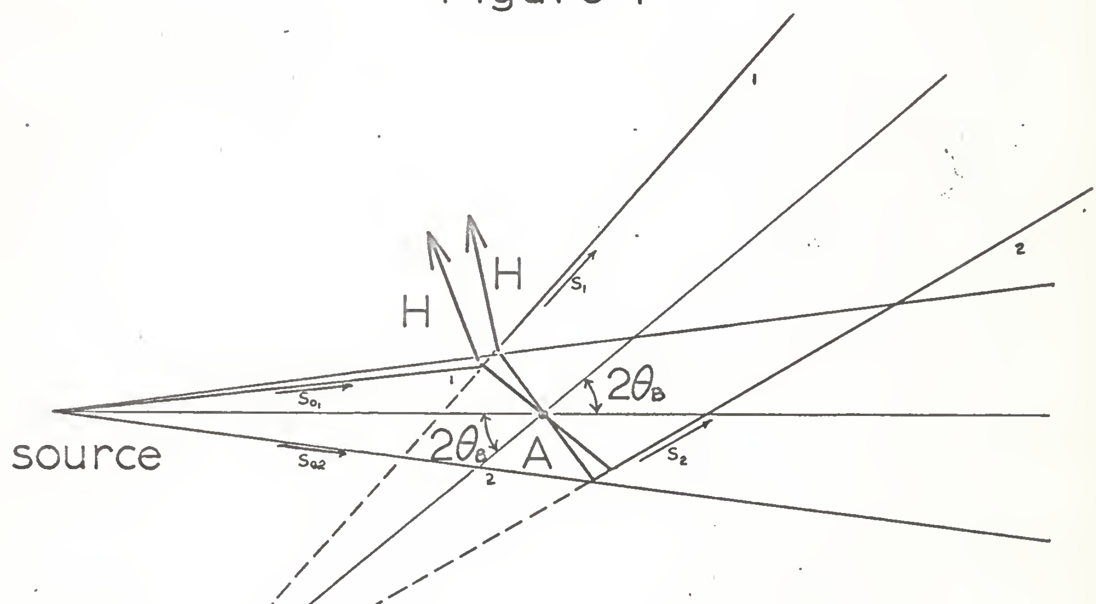

Figure 2

crystal about its axis and the motion of the diffracted beam about the virtual source can be mechanically connected. A system of slits may be set to rotate about the virtual source through an angle equal to that of rotation of the crystal. The slits would accurately track the diffracted beam for small angles of rotation. Such slits could be used to cut out background and possibly extraneous characteristic radiations.

There will be a magnification factor applying to the topograph arising from the rotation of the sample. This is in addition to the magnification already existing in the direction parallel to the diffracting planes. The factor arising in the rotation is perpendicular to the diffracting planes. These combine to provide an overall magnification of the image. The magnification factor due to rotation depends on the angle the diffracting planes make with the surface and the distance to the film.

Stereo pairs may be taken easily with the idealized apparatus shown in Plate III. The opposite side of the same set of planes may be used. The only change in apparatus involved is a rotation of the crystal and a change in position of the film.

The resolution of the camera is limited by two principal factors. These are the vertical divergence and the focusing of the diffracted beam. The vertical divergence has been discussed as it applied to the Lang experiment. The same effect holds true for this camera. The camera was constructed so that the film to crystal distance was equal to the source to crystal distance. The size of the image of the source at the film position will be equal to the size of the source itself.

A more serious resolution problem is that of the focusing of the diffracted beam. If the sample is large enough two of the characteristic radiations may diffract from different positions in the crystal. For a crystal with the diffracting planes oriented perpendicular to the face, all of the diffracted radiation will converge to a point. The point is at a distance behind the crystal equal to the source to crystal distance. The focusing also makes it difficult to eliminate unwanted characteristic radiations by using slits. In general the K_β will be filtered out and the K_{α_1} and K_{α_2} will be allowed to reach the film. The separation of the two diffracting positions within the crystal is on the order of 20 to 50 microns.

The loss of resolution due to the focusing of the diffracted beam can be calculated. This will be done for the simplest case. That is for a crystal cut with the diffracting planes normal to the face. This is sufficient because crystals cut otherwise will give the same effect with an indistinct focus. The effect is illustrated in Fig. 4. The angles θ_1 and θ_2 are the Bragg angles for two wavelengths present in the incident beam. The distance R is the source to crystal distance. The distance d_0 is the separation of the diffracting positions in the crystal. The value d_0 is given by the difference $R\tan\theta_1 - R\tan\theta_2$.

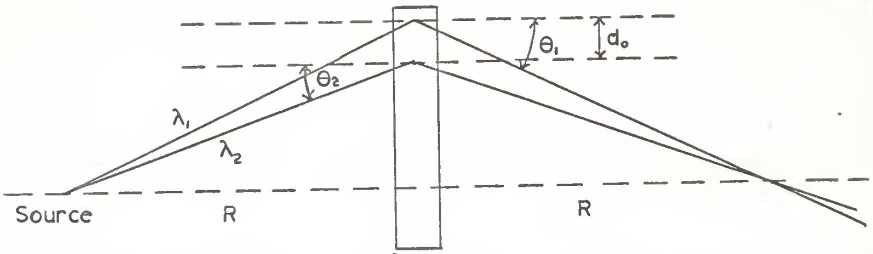

Fig. 4

An additional limiting factor on the resolution occurs with the rotation of the crystal in the divergent beam. A single point within the crystal will give a smeared out image on the film. The effect may be understood by examining Figs. 5a and 5b. The point P(x,y) in Fig. 5a is just in position for diffraction. As the crystal is rotated through a small angle n, as seen in Fig. 5b, the diffracting zone will translate. The point P(x,y), however, will be in the portion of the crystal transversed by the diffracted beam. The loss of resolution occurs as the diffracted beam passing through the point moves across the film. A derivation of the magnitude of the effect is given in the Appendix.

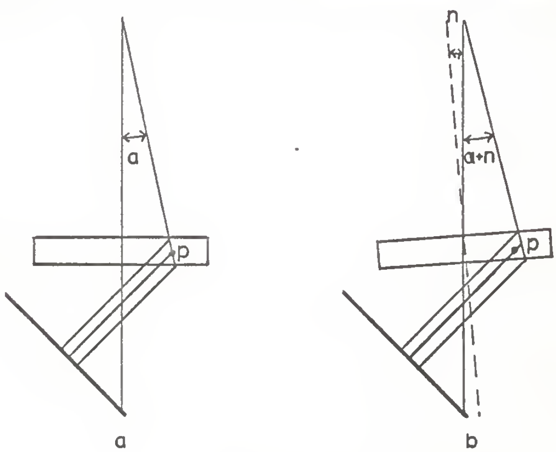

Fig. 5

CONSTRUCTION OF THE CAMERA

The unit was constructed as shown in Plate IV. This is a graphic drawing of the camera showing the principal features. Plate V shows two photographs of the apparatus. An associated component was constructed for alignment purposes. It includes a mount for a GM tube which pivots on a small table below the center of symmetry of the camera. Diffraction angles may be measured on the table. A collimating slit system and shutter are mounted on the table.

The crystal is mounted on a single crystal goniometer which is attached to a sleeve. This sleeve can be rotated about a shaft which is attached to a central wheel. The sleeve and goniometer can be raised and lowered by means of a central screw. The position desired is maintained by a locking screw through the sleeve. The goniometer mount, including shaft, sleeve and wheel, is free to rotate about a vertical axis through the plate. The plate and goniometer may then be mounted so that the crystal is in the direct beam of the microfocus unit.

The open semicircle has its center at the goniometer mount and serves as the guide for the film holder. The film holder locks in position by means of two one inch screws passing through the plate. The film is held in a light tight pack and is slipped into the slot in the film holder.

The slit system is mounted on the closed semicircle. The unit is positioned so that both the source point focus and the

EXPLANATION OF PLATE IV

Fig. 1 A side view of the camera described in this report showing the cam holder, goniometer mount, film holder and slit.

Fig. 2 A top view of the camera showing the cam, drive belt, and position of the film holder.

PLATE IV

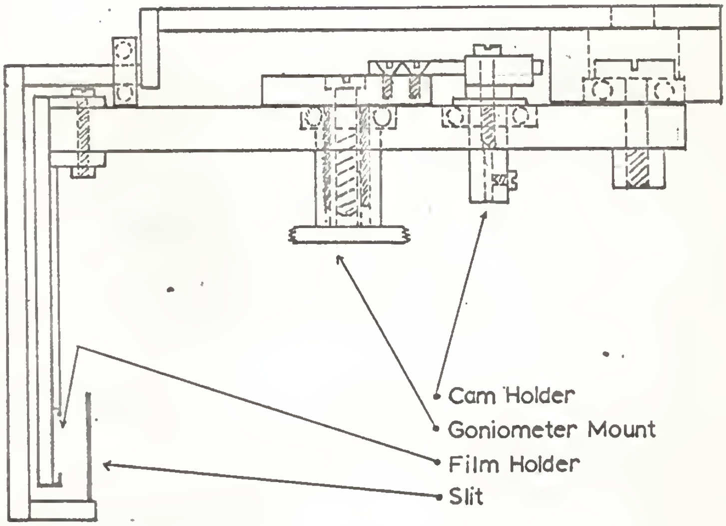

Figure 1

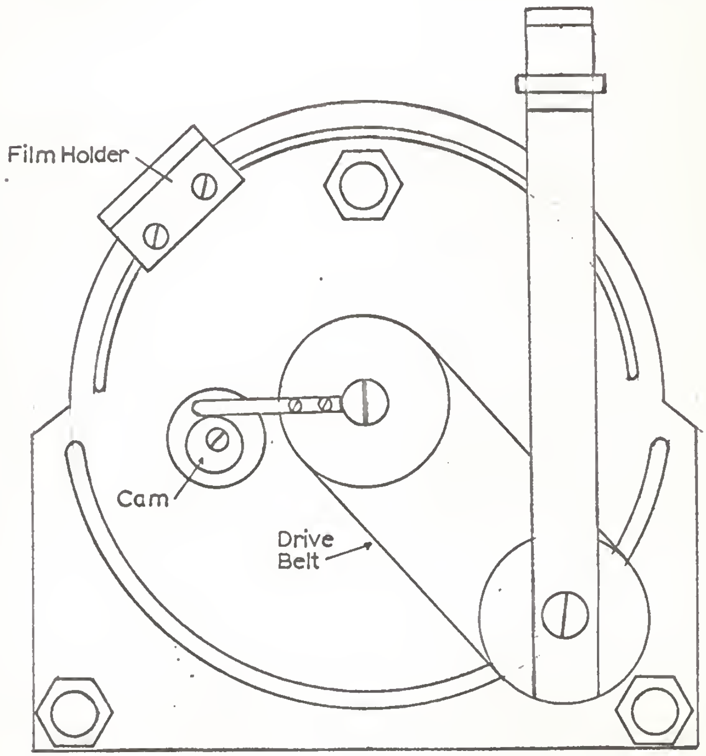

Figure 2

EXPLANATION OF PLATE V

Fig. 1 A side view of the camera described in this report. The drive motor is seen to the right of the porcelain socket. The Geiger tube extends to the left from the alignment table. The goniometer is seen directly above the thumbscrew in the alignment table.

Fig. 2 A view of the camera from above showing the count-rate meter and Geiger tube. Other parts may be identified by comparing this photograph with the drawings in Plate IV.

PLATE V

Figure 1

Figure 2

virtual source lie on this closed semicircle. The slit system is mounted on an arm which extends around the film holder. It is supported by a roller bearing and is attached to a wheel at the position of the virtual source. This wheel and the wheel at the center have the same radius. A shim steel belt is used to coordinate the motion such that the slit moves through the same angle as the crystal.

The whole unit is driven by a 6 cycle per hour electric motor. A cam is attached to the shaft of the motor. An arm is held under tension on the cam. For uniform motion the cam should be in the shape of a cardioid. This sort of cam is difficult to build accurately. The material should be hard enough to take the wear that is to be expected. A substitute shape was used. This was a small ball bearing that was frozen with a drop of solder. The bearing was displaced from the center of the motor axis. The pictures obtained are uniform except at the turning points.

The table shown below the camera was built primarily to detect the position of the diffracted beam. The arm holds an end window GM tube which was used with a count rate meter. The center of the table is directly below the axis of the goniometer mount. Angle markings on the table enable one to accurately position the counter where the diffracted beam is expected. A system of slits is mounted on the table to cut out extraneous radiation. The table is shaped so that the direction of the incident beam is given on the table when the table is mounted flush to the face of the x-ray tube. The slit system also includes a shutter which may be operated from a safe distance.

The alignment for a small crystal will be described. Once the orientation of the crystal is known it is mounted on the single crystal goniometer and the unit is placed over the center of the alignment table. The crystal can be adjusted to the same level as the source and film pack. The counter is positioned at the expected angle of emergence of the diffracted beam. The 6 cycle/hr motor is turned on and the diffracted beam is allowed to scan a piece of low resolution x-ray film for one cycle. This is developed and the width of the scan is measured. If it is not more than twice the width of the whole sample the whole sample will not be in the topograph. The cam is displaced more from its axis to obtain a wider scan. Generally only part of the crystal is in position to diffract during the scan. The alignment topograph will show only part of the crystal. The crystal is then properly aligned by rotating it slightly into the beam and taking another one cycle scan. This is continued until the crystal image is centered on the topograph. A high resolution film such as Kodak AA is used for the final exposure.

EXPERIMENTAL RESULTS

The focusing of the diffracted beam, which is a major cause of loss of resolution, was detected and measured.

Plate VI shows a series of exposures taken at equal intervals of distance from the crystal through the film position. The crystal used was a calcium carbonate (calcite) cleavage plate. The radiation used was the continuous band of Ag. Each exposure was taken for 10 minutes. The series shows clearly how all wavelengths converge at the proper film position as designed for this unit.

Sample crystals used were Si, $CaCO_3$, and Alpha Quartz. The combination of radiation and crystal was determined by the criterion expressed earlier. The value of μt must be less than unity. Below, in Table 1, the values of μ are calculated for the various combinations of crystal and radiation.

Table 1 Values of the Linear Absorbtion Coefficient, μ (cm^{-1})

Crystal	AgK_α $\lambda = 0.56A$	MoK_α $\lambda = 0.71A$	CuK_α $\lambda = 1.54A$
Si	8.03	15.6	141.
SiO_2	5.46	10.4	92.5
$CaCO_3$	- - -	23.7	206.

The inverse of each value of μ gives the upper limit on the thickness of the crystal for a given radiation. These are listed in Table 2.

The results of two of these combinations will be reviewed. They are the Quartz-MoK_α combination and the Calcite-CuK_α combination.

EXPLANATION OF PLATE VI

Plate VI The divergence of the diffracted beam. The photographs are 3.7X enlargements of ten minute exposures taken at equal intervals of distance along the beam.

PLATE VI

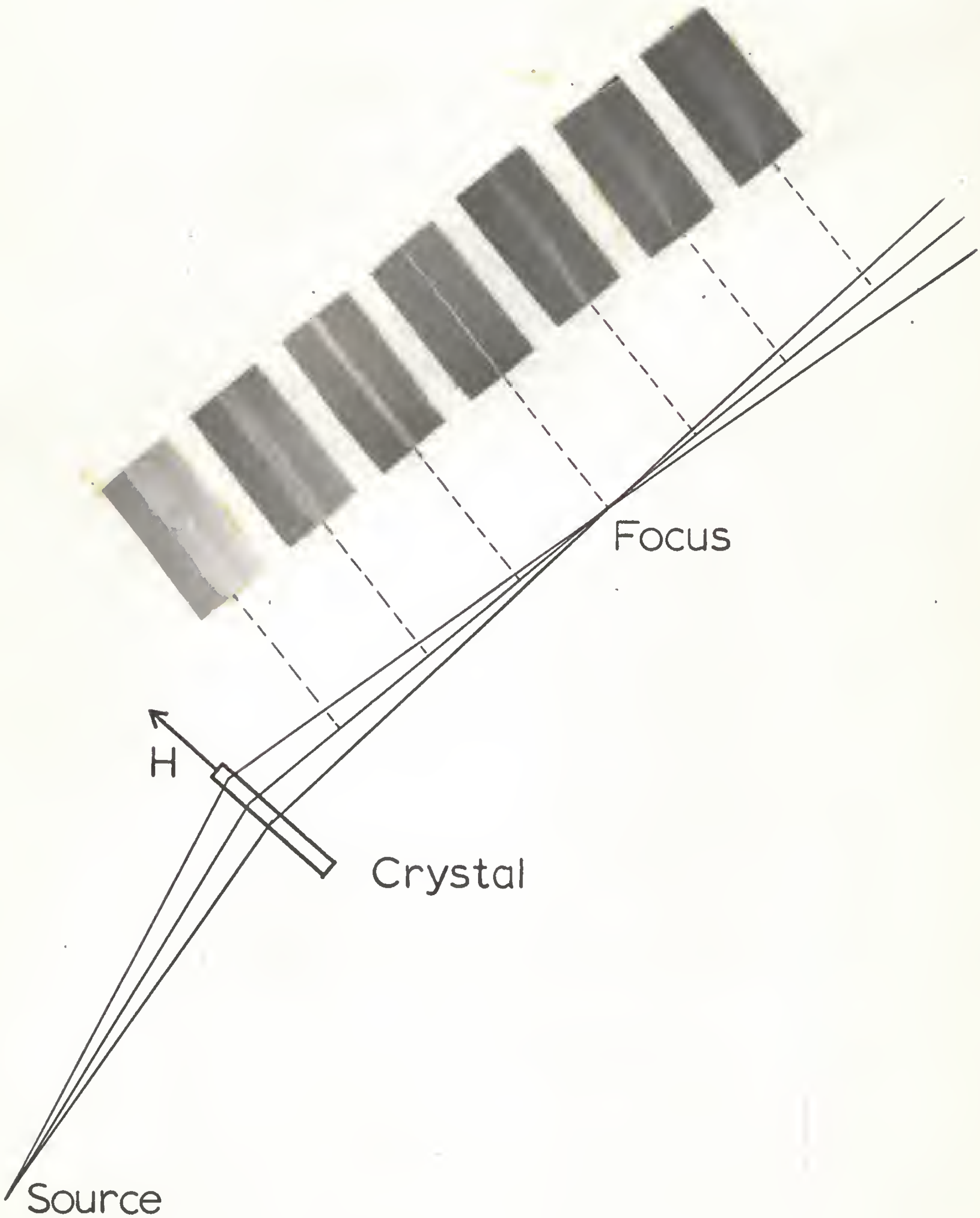

Table 2 Upper Limits on the Thickness of Crystals (cm)

Crystal	AgK_α $\lambda = 0.56A$	MoK_α $\lambda = 0.71A$	CuK_α $\lambda = 1.54A$
Si	.125	.064	.0071
SiO_2	.183	.098	.011
$CaCO_3$	- - -	.042	.0049

The main objective in using the combination of quartz and MoK_α was to verify that the method gave the same results as obtained in the Lang method. An Alpha quartz sample was given to us by Dr. W. J. Spencer of Bell Telephone Laboratories. The sample was grown artificially. A Lang topograph of the crystal was published in a report by Dr. Spencer. This was supplied to us with the crystal for comparison with topographs obtained with this camera. It is seen in Plate VII, Fig. 1.

The Lang photograph was made using AgK_α radiation with tube being operated at 50 KV. Our microfocus unit operates at approximately 35KV. It was found that the K_α line of Ag was not sufficiently intense with respect to the continuous spectrum for this voltage. The 35KV was sufficient to excite the MoK_α line. This was used to make our topographs of the quartz sample. Less contrast is to be expected with the combination of MoK_α and quartz. This is true because the value of μt for the MoK_α -SiO_2 combination is larger than for AgK_α -SiO_2.

The (11·0) planes were used for diffraction. These are the same planes used for the Lang topograph. An exposure time of 7 hours on Kodak AA film was used. A stereo pair was taken of one portion of the crystal. The results are seen in Plate

EXPLANATION OF PLATE VII

Fig. 1 The topograph of the quartz plate made by the Lang method. Published in a Bell Telephone Laboratories Report.

Fig. 2 A topograph of the same quartz plate made by the camera described in this report. The magnification is 3.6X the crystal.

Fig. 3 The other half to the stereo pair of the section of crystal shown in Fig. 2. The magnification is 3.6X the crystal.

Fig. 4 and Fig. 5 A stereo pair of a very thin calcite single crystal. The magnification is 10.8X the crystal.

PLATE VII

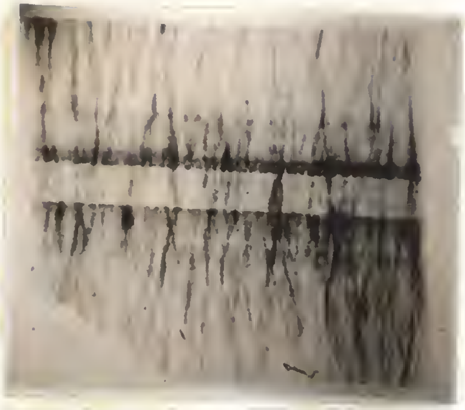

Figure 1

Figure 2

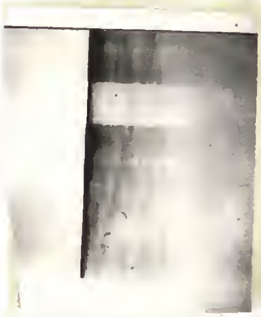

Figure 3

Figure 4

Figure 5

VII, Figs. 2 and 3. Enough similarity between the Lang topograph and the one obtained by rotation can be found to verify that the camera is capable of obtaining x-ray diffraction topographs. The stereo pair was viewed in a stereo viewer. No outstanding three dimensional effect was seen. This is due to the large viewing angle (about 17°) and the lack of sharp detail.

The calcite-CuK_{α} combination was used because calcite is nearly dislocation free, can be prepared very thin, and because CuK_{α} radiation is excited very strongly at 35KV. Results of calcite topographs have been published by Lang[1]. These can be used as a check on the camera.

A cleavage slice of calcite was sanded and etched in dilute HCl until it was less than .05mm in thickness. The cleavage planes were used for diffraction. They make an angle of 75.5° with the surface. This has the effect of moving the focus out of the plane of the film. The K_{α_1} and K_{α_2} will give two slightly displaced images at the film position.

A stereo pair was taken. They are shown in Plate VII, Figs. 4 and 5. The double images may be seen. Details very similar to those observed in the ones obtained by Lang are seen. The heavy dark lines are identified as dislocations. The series of fine lines above the heavy ones were seen by Lang but not identified. These seem to be peculiar to calcite. The difference between the two topographs in the pair is easily seen. They are difficult to view in a stereo because of the large viewing angle involved. This angle is 28.4° for the calcite-CuK_{α} combination.

CONCLUSIONS AND EVALUATION OF THE CAMERA

The technique of rotating the crystal in a divergent beam to obtain a topograph has several advantages over the translation method. The alignment is simple if the orientation of the crystal is known. The principal advantage in alignment is the insensitivity of the technique to curvature of the sample. The Lang technique is very sensitive to curvature of the sample. The strain between two crystal mounts is often enough to cause part of the topograph to be lost. This does not occur in the rotation method because of the method of plane selection by the divergent beam. If the crystal was curved before mounting a topograph could still be obtained. The method may be useful in the examination of deliberately bent crystals. An adjustment on the moving slit mechanism would have to be made.

The magnification factor which is inherent in the rotating system does not exist in the translation method. A magnification factor could be obtained in the translation method by placing the film at a larger distance from the crystal. This would result in decreased resolution and increased exposure times. Also, the magnification would only be in one dimension. For low Bragg angles the rotation method provides the same magnification factor in both dimensions of the film.

There are disadvantages in the rotating crystal technique.

The loss of resolution due to the simultaneous diffraction of the K_{α_1} and K_{α_2} lines is the principal drawback. Although detail is not lost the topographs give less information because each line gives a picture. These are superimposed on the film. This is effectively a loss of resolution and is the principal cause of low resolution in the camera. This is serious enough to prevent the use of the camera for high resolution studies of individual dislocations.

The loss of resolution due to rotation of the crystal in a divergent beam does not appear to be a serious problem. This effect would have to be investigated further for thicker crystals. As is shown in the Appendix the effect depends in a specified way on the Bragg angle and the thickness of the crystal. The resolution should increase for a smaller Bragg angle and for thinner samples.

The size of the sample is limited for short wavelengths. For short wavelengths the Bragg angle is small and may be less than twice the angle of divergence of the incident beam. For this case the diffracted will remain in the path of the incident beam and it will be impossible to obtain a topograph. To avoid this the angular divergence of the incident beam must be limited. This limits the area of the crystal which can be viewed at these small Bragg angles.

Stereo pairs can be taken more easily with the rotation camera. There is no need to remount the crystal for a second picture. This is a problem in the Lang method because of the chance of breakage during remounting.

A comparison of exposure times is difficult to make. The microfocus unit was operated at 35KV. The 35KV was not sufficient to excite the Ag lines strongly over the continuous background spectra. This is the radiation used most frequently by other investigators. If the camera was to be used effectively, careful calculations should be made on the loss of resolution due to rotation of the sample. This would have to be done for thick samples. A strong source of short wavelength radiation is needed to improve resolution and contrast. If the alignment procedure was very simple and if exposure times were small, the method could be used for rapid testing of perfection of crystals.

ACKNOWLEDGMENT

The author wishes to express his gratitude to Dr. R. Dean Dragsdorf for initiation of the problem and for his guidance through the problem. Appreciation is also expressed to Dr. Glen E. Harland for instruction in the use of the microfocus unit, to Mr. L. W. Philips for his assistance in the construction of the camera and to Dr. W. J. Spencer for use of his quartz crystal.

This research was sponsored by the Bureau of General Research, Kansas State University. The author wishes to thank this group for the research assistantship under which this work was carried out.

REFERENCES

(1) Lang, A. R.
Studies of Individual Dislocations in Crystals by X-Ray Diffraction Microradiography. J. Appl. Phys., 30:1748. 1959.

(2) Lang, A. R.
The Projection Topography: A New Method in X-Ray Diffraction Microradiography. Acta Cryst., 12:249. 1959.

(3) Lang, A. R.
Direct Observation of Individual Dislocations by X-Ray Diffraction. J. Appl. Phys., 29:598. 1958.

(4) Jenkinson, A. E.
Projection Topographs of Dislocations. Philips Tech. Rev., 23:82 1961/62

(5) Newkirk, J. B., and J. H. Wernick, Editors
Direct Observations of Imperfections in Crystal. Interscience Publishers, New York, 1962.

APPENDIX

RESOLUTION LOSS DUE TO ROTATION

A resolution loss occurs due to the rotation of the crystal in the divergent beam. The effect results in a smeared out image perpendicular to the diffracting planes. The calculation of the loss of resolution is given here with the aid of the diagrams in Plate VIII.

The crystal sample is placed normal to the axis of the incident cone of radiation. The diffraction planes are at an angle α with respect to the normal to the crystal face. The film is placed at an angle ϵ with respect to the axis of the incident beam. The point to be considered has the coordinates (x,y) within the source. The value of y is measured into the crystal perpendicular to the face. The distance from the source to the origin is A. The distance from the origin to point 2 is B. Other distances and angles are indicated in the figures in Plate VIII.

The point (x,y) in Fig. 1 is just in position for diffraction. The normal to the crystal face is set at an angle of η_1 with respect to the axis of the cone of radiation. As the crystal is rotated through a small angle to the angle η_2, as is seen in Fig. 2, the diffracting zone will translate across the crystal. One point in particular will be diffracting so that the original point (x,y) is in the diffracted beam. Throughout the rotation the point (x,y) will be causing a disruption of extinction in the diffracted beam is this point is in a region of imperfection in the lattice. Increased intensity will be seen on the film at several points due to the single point in the crystal. This is the loss of resolution that will be calculated.

The change in position of the image of the point on the film, $\triangle q$, is given by $q-q'$.

From Fig. 1 the following relations are derived.

$$\frac{\sin(\theta+\alpha-\eta_1)}{q'} = \frac{\sin(180^\circ-\theta-\alpha+\eta_1-\epsilon)}{B_{12}}$$

$$\frac{\sin(90^\circ-\theta-\alpha)}{B_{10}} = \frac{\sin(\theta+\alpha-\eta_1)}{x+y\tan(\theta+\alpha)}$$

$$B_{10}' = \frac{\cos(\theta+\alpha)[x+y\tan(\theta+\alpha)]}{\sin(\theta+\alpha-\eta_1)}$$

$$B_{12} = B - B_{10}$$

From Fig. 2 the following relations are derived.

$$\frac{\sin(\theta+\alpha-\eta_2)}{q} = \frac{\sin(180^\circ-\theta-\alpha+\eta_2-\epsilon)}{B_{12}'}$$

$$\frac{\sin(90^\circ-\theta-\alpha)}{B_{10}'} = \frac{\sin(\theta+\alpha-\eta_2)}{x+y\tan(\theta+\alpha)}$$

$$B_{10}' = \frac{\cos(\theta+\alpha)[x+y\tan(\theta+\alpha)}{\sin(\theta+\alpha-\eta_2)}$$

$$B_{12}' = B - B_{10}'$$

EXPLANATION OF PLATE VIII

Fig. 1 The crystal is set so that the normal to its face makes an angle of n_1 with the axis of the incident cone of radiation. q' gives the position on the film of the image of the diffracting point (x,y).

Fig. 2 The crystal is rotated to a new angle n_2 with respect to the source. Diffraction is occurring from points behind the point (x,y). The new position of the image of point (x,y) is given by q.

PLATE VIII

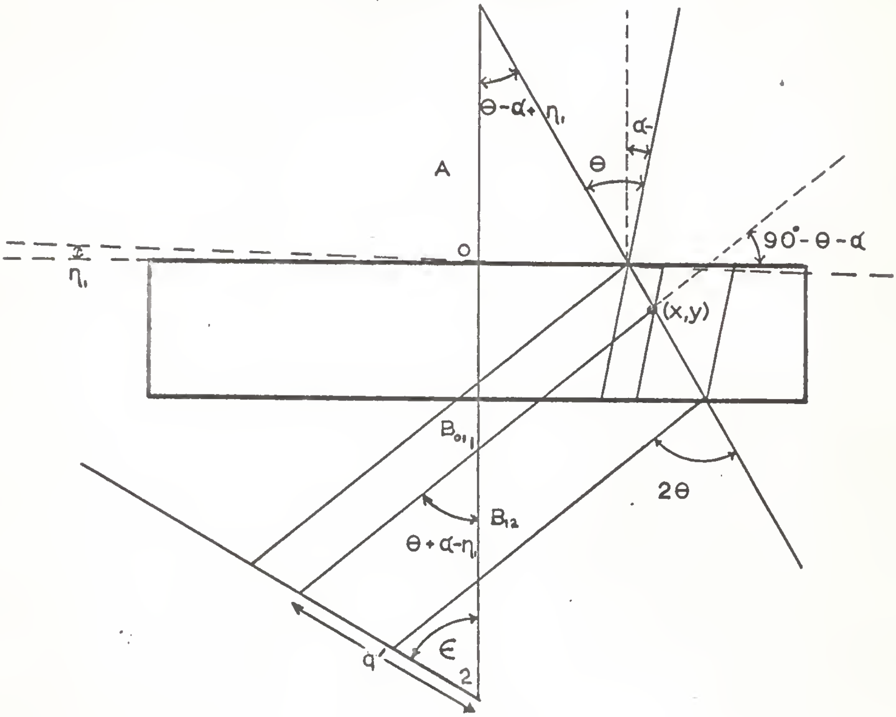

Figure 1

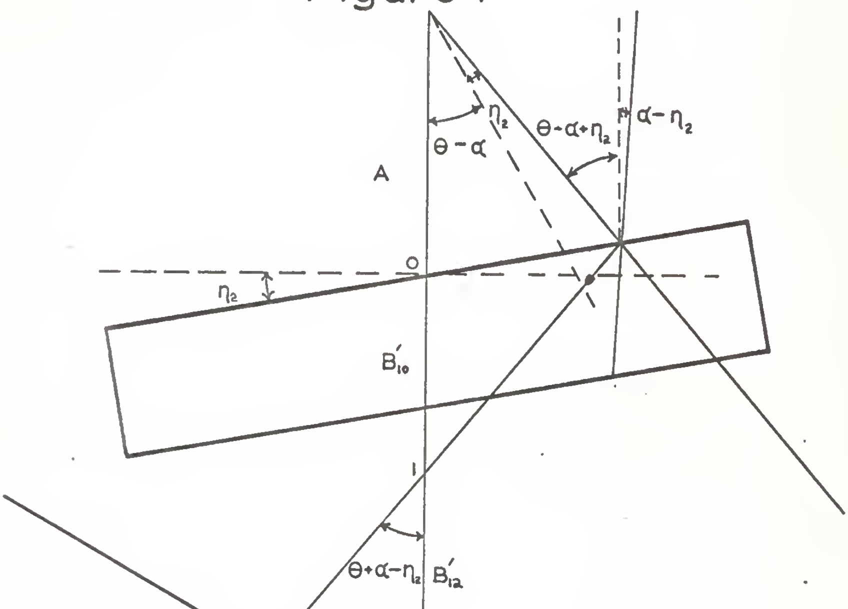

Figure 2

The difference between q, the initial position on the film, and q', the final position on the film, is given below.

$$\Delta q = q - q' = \frac{B_2' \sin(\theta + \alpha - \eta_2)}{\sin(\theta + \alpha + \epsilon - \eta_2)} - \frac{B_1 \sin(\theta + \alpha - \eta_1)}{\sin(\theta + \alpha + \epsilon - \eta_1)}$$

Application of trigonometric identities reduces this form to:

$$\Delta q = \frac{B \sin(\eta_1 - \eta_2) \sin(\epsilon)}{\sin(\eta_1) \sin(\eta_2) + \sin(\theta + \alpha + \epsilon) \sin(\theta + \alpha + \epsilon - \eta_1 - \eta_2)} +$$

$$\left[x \cos(\theta + \alpha) + y \sin(\theta \pm \alpha)\right] \left(\frac{1}{\sin(\theta + \alpha + \epsilon - \eta_1)} - \frac{1}{\sin(\theta + \alpha + \epsilon - \eta_2)} \right)$$

Figures 1 and 2 are used to derive values of q' and q, respectively. Relations are still needed which give the angles η_1 and η_2 as a function of the initial and final diffracting points. These are obtained from Figs. 1 and 2 by using the law of sines.

The relation for η_1 is obtained by reducing

$$\frac{\sin(\theta - \alpha + \eta_1)}{x_1 - y_1 \tan(\theta - \alpha)} = \frac{\cos(\theta - \alpha)}{A}$$

to

$$\tan(\theta - \alpha) = \frac{x_1 - A \sin(\eta_1)}{y_1 + A \cos(\eta_1)}$$

The relation for η_2 is obtained by reducing

$$\frac{\sin(\theta - \alpha + \eta_2)}{x_1 + y_1 \tan(\theta + \alpha)} = \frac{\cos(\theta - \alpha)}{A}$$

to

$$x_1 + y_1 \tan(\theta + \alpha) = A\left[\tan(\theta - \alpha) \cos(\eta_2) + \sin(\eta_2)\right]$$

Having measured the thickness of the crystal, it is possible to calculate the values of η_1 and η_2 for same diffracting position in the crystal.

A calculation of this type was carried out for the quartz sample from Bell Telephone Laboratories. For our experimental arrangement the following values were applicable:

$A = 8.89$cm, $\theta = 8.30°$, $\alpha = 0°$, and $\epsilon = 90° - 2\theta$. The thickness of the crystal was 0.3mm. A value of 0.1mm was used in the calculations for the thickness. The value of x_1 was 5mm. This corresponds roughly to a desired experimental arrangement. The value of η_1 was found to be 1.156. The value of η_2 was found to be 1.158. When these were used in the form given for Δq, a value of 3 microns was obtained. A checking calculation using the values $x_1 = 0.1$mm and $y_1 = 0.3$mm was made. This was done to check the magnitude of the result and to test the dependence of Δq on thickness. The final value of Δq obtained was 8 microns. This is not a significant loss of resolution as dislocation images are generally 20 microns in width.

DESIGN AND EVALUATION OF A NEW X-RAY DIFFRACTION TOPOGRAPH CAMERA

by

MARK JEROME DREILING

B. S., Kansas State University, 1962

AN ABSTRACT OF A THESIS

submitted in partial fulfillment of the

requirements for the degree

MASTER OF SCIENCE

Department of Physics

KANSAS STATE UNIVERSITY
Manhattan, Kansas

1964

An x-ray diffraction topograph camera is designed which uses to advantage the divergent beam available in a microfocus unit. A single crystal is rotated about an axis perpendicular to the axis of the incident cone of radiation. A system of slits, which is linked mechanically to the rotation of the crystal, tracks the diffracted beam. A manification factor in both dimensions of the topograph image is inherent in the system. Remounting of the sample is unnecessary to obtain stereo pairs because of the rotational symmetry. A rotation of the crystal through twice the Bragg angle and a change in position of the film pack is necessary to obtain the stereo pair. The camera is insensitive to curvature in the sample. This is a result of the method of plane selection. The planes are selected by the divergent beam originating at a point source.

The resolution is limited by three factors. The vertical divergence occurs in the same manner as in the Lang method. The resolution in the vertical direction is limited to 20 microns by the vertical divergence. The resolution is limited because the whole crystal is exposed to the divergent beam. The K_{α_1} and K_{α_2} characteristic radiations diffract from two closely spaced positions in the crystal. The two diffracted beams focus to a point behind the crystal. The loss of resolution depends on the crystal used, the wavelength, and the difference in wavelength of the K_{α_1} and K_{α_2} . A third cause of loss of resolution occurs in the rotation of the crystal in the divergent beam. A single point in the crystal is in the diffracted beam over a certain arc of rotation. During this rotation the diffracted beam is affected by the loss of extinction at the point. A line on the film corresponds to a point in the crystal. The magnitude of this effect has been calculated. It is not significant for the samples used in this experiment. The loss of resolution due to rotation increases with the thickness of the sample and may be critical for samples which have a thickness greater than one centimeter. Loss of resolution due to horizontal divergence is negligible because of the small size of the source.

A topograph was made of an alpha quartz plate. This topograph was compared with a topograph of the same crystal made with the Lang method. The similarity between the two topographs justified further investigation of the rotation method. Limitations in the x-ray equipment prevented a careful comparison of the results of the two methods. Silver characteristic radiation was used for the Lang topograph. A limitation on the accelerating voltage required that MoK_α characteristic radiation be used for the rotation topograph. Contrast and resolution are improved for the shorter wavelength. Exposure times were dependent on the wavelengths used and the thickness of the crystal. A satisfactory topograph was obtained of a 0.36mm thick, 3.5mm wide section of the quartz sample. The exposure time was 7 hours with MoK_α radiation and an accelerating voltage of 35KV.

Further work is in progress to determine camera configurations which provide improved resolution and shorter exposure times.